EFFECTS OF SODIUM EXPOSURE ON GRADE 91 STEEL

Y. Chen, Z. Zeng, and M. Li
Argonne National Laboratory
Lemont, IL, USA

Email contact of corresponding author: Yiren_chen@anl.gov

ABSTRACT

To assess the performance of Grade 91 (G91) steel in sodium-cooled fast reactors (SFR), the corrosion behavior and mechanical properties of G91 were evaluated with sodium-exposed and thermally aged samples. The sodium-exposure experiments were carried out with flat tensile samples in forced convection sodium loops between 550 and 650°C. The thermal-aging experiments were conducted at the same temperatures in vacuum. While the effect of sodium exposure was insignificant at 550 and 600°C, the yield stress and ultimate tensile strength declined considerably after the exposures at 650°C. The reduction in tensile strength was accompanied by the dissolution of $M_{23}C_6$ carbides and excessive grain growth in G91. The thermodynamic analysis suggested that NbC and VC may play an important role in stabilizing the alloy's microstructure in low-carbon-activity environments, critical for the decarburization resistance of G91.

INTRODUCTION

The Sodium-cooled Fast Reactor (SFR) is an advanced reactor concept with high technical maturity. Building upon the previous experience with experimental SFRs, a solid knowledge base has been established to guide future development [1]. A critical aspect of the research on SFR is reactor structural materials that can come into direct contact with liquid sodium. The choice of suitable materials is essential to ensure the long-term integrity and optimal performance of SFR. While liquid sodium has significant advantages as a reactor coolant thanks to its excellent thermal properties, it can also interact with reactor structural materials at elevated temperatures, leading to microstructural instabilities and property deteriorations. The interactions between structural alloys and liquid sodium can be broadly classified into two categories -- the transfers of metallic and nonmetallic elements across the alloy-sodium boundary. The transfer of metallic elements is a dissolution process. Depending on the solubility in sodium, alloy elements can be dissolved uniformly or preferentially into liquid sodium, forming surface corrosion products that can subsequently be eroded or spalled into flowing sodium [2][3]. The transfer of nonmetallic elements involves oxygen, carbon, and nitrogen in the alloy-sodium system. As a result of different chemical activities, mass transfers of these elements can occur in isothermal or non-isothermal systems, and among materials with different compositions. By examining the partitioning of nonmetallic elements between the structural alloy and sodium, the extent to which oxygen, carbon, and nitrogen interact in the structural material-sodium systems can be assessed.

Grade 91 (G91) is an advanced structural material with great potential for SFR applications. Initially developed in the US for intermediate heat exchangers and steam generators of liquid metal reactors, G91 shows excellent creep properties, good corrosion resistance, and high thermal conductivity. As a ferritic-martensitic steel, it is also more resistant to swelling compared to austenitic stainless steels under irradiation. Over the years, considerable information has been accumulated for G91 through various Department of Energy (DOE) and

industry-sponsored programs. An extensive database of mechanical properties for G91 has been established. However, data for G91 exposed to liquid sodium are scarce, and consequently, the knowledge of the long-term performance of G91 in sodium is still limited. In the meantime, carburization or decarburization of G91 in sodium is also unclear because the migration of carbon in the G91-sodium system has not been fully understood. In this study, the effects of sodium exposure on the microstructural stability and tensile properties of G91 steel were investigated. The sodium-exposure conditions that can lead to carburization or decarburization of G91 were evaluated.

EXPERIMENTAL

Two heats of G91 steel, H1 and H30176, were included in this study. The chemical compositions of these two heats are shown in Table 1. Heat H1 was an archive material from a previous research program. The material was a plate of 9.5-mm thick, and was normalized at 1050°C and tempered at 760°C for 1 h before being air cooled to room temperature. Heat H30176 was also a plate about 25-mm thick, and was normalized at 1050°C for 1 h and tempered at 760°C for 2 h. After the heat treatments, Heat 30176 was also air cooled to room temperature.

Table 1. Chemical composition (wt.%) and heat treatment for Heats H1 and H30176

Heat ID	C	Cr	Mn	Mo	N	Nb	Si	V	W	Heat treatment
H1	0.09	8.3	0.46	1.04	0.06	0.05	0.41	0.22	-	1050°C 1 h + 760°C 1 h
H30176	0.08	8.6	0.37	0.89	0.06	0.07	0.11	0.21	<0.01	1050°C 1 h + 760°C 2 h

The specimens used in this study have a sub-sized, sheet-type design with a nominal gauge length of 7.6 mm, a width of 1.5 mm, and a thickness of 0.76 mm. The specimens were sectioned from the plates with their tensile directions parallel to the rolling directions. All post-exposure corrosion, mechanical, and microstructural evaluations were conducted with the same specimens to avoid any ambiguity.

Sodium-exposure experiments were performed in two forced convection sodium loops. Three test vessels operating at 550, 600, and 650°C, respectively, were used for sodium exposure. For each temperature, the samples were loaded on sample holders and inserted into the test vessel. During the exposure experiments, the oxygen content in sodium was controlled with the cold trap whose temperature was kept at ~120°C. Restricted by the oxygen solubility at the cold-trap temperature, the oxygen concentration in sodium was maintained at ~1 wppm during the tests [4]. In parallel with the sodium-exposure tests, thermal aging experiments were performed at the same temperatures. The objective of thermal aging experiments was to assess the response of G91 to thermal exposure in a non-reactive environment, providing insights into degradation mechanisms.

After the sodium-exposure experiments, the samples were retrieved from the test vessels, cleaned, weighed, measured for thickness. The weight and thickness changes resulting from sodium exposures were used to assess the corrosion performance. Tensile tests were also performed with the sodium-exposed and thermally aged specimens to assess their mechanical response. The tests were performed in an electromechanical testing system equipped with a three-zone air-atmosphere furnace. For each specimen, the tensile test temperature was identical to its sodium-exposure or thermal-aging temperature. All tests were performed with a nominal strain rate of 0.001 s^{-1}.

RESULTS AND DISCUSSION

Weight losses were observed in G91 after sodium exposures at 550, 600, and 650°C. With the weight data before and after sodium exposures, corrosion rates were estimated at different temperatures. The corrosion rate of G91 decreased with increasing exposure time and reached a steady state after ~10,000 h. Fig. 1 shows the corrosion rates of G91 after reaching the steady state. The average corrosion rates were about 0.1, 0.2, and 0.3 μm/y at 550, 600, and 650°C, respectively. The solid and dashed lines in the figure are the calculated results with Eq. (1) from reference [5] (also known as Monju formula) for oxygen contents, 0.1, 1, and 5 wppm.

$$log_{10}R = 0.85 + 1.5log_{10}C_0 - \frac{3900}{T+273}, \quad (1)$$

where R is the corrosion rate in μm/y, C_0 is the dissolved oxygen in wppm, and T is the temperature in °C. It appears that the Monju formula is applicable to G91 steel.

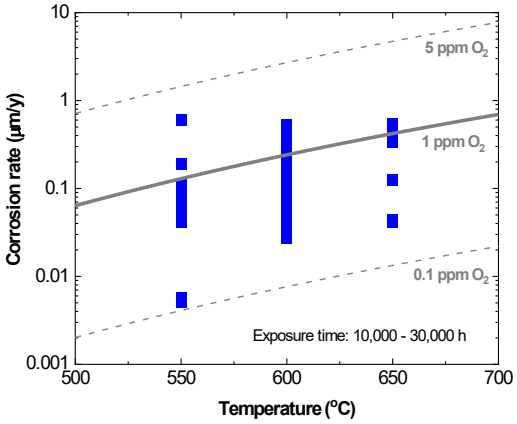

Fig. 1. Corrosion rate for G91steel exposed to sodium at 550, 600, and 650°C. The solid and dashed lines are the calculated corrosion rates for the oxygen levels of 0.1, 1, and 5 wppm.

Uniaxial tensile tests were performed before and after sodium exposure or thermal aging experiments. Fig. 2 shows the engineering stress-strain curves of Heat H1 in as-received, and selected thermally aged, and sodium-exposed conditions. As expected, the tensile behavior of G91 was sensitive to test temperature. Both yield stress and ultimate tensile strength declined monotonically with the increasing test temperature. The uniform and total elongations decreased from room temperature to 400°C, but increased continuously from 400 to 650°C. The two G91 heats with different temper time (1 h vs. 2 h) did not lead to any obvious difference in their tensile responses.

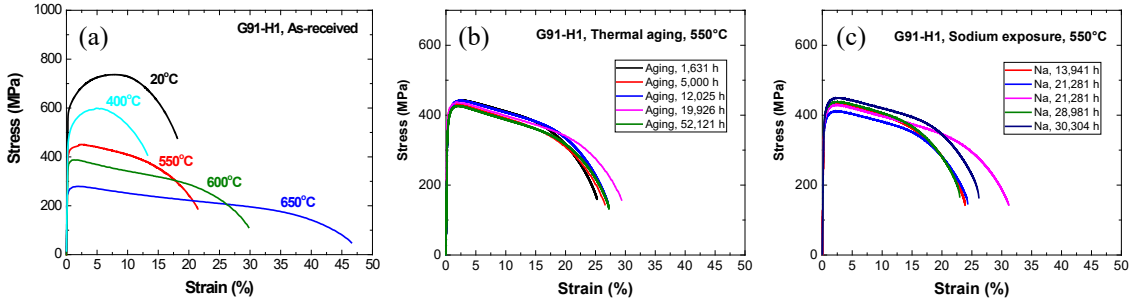

Fig. 2. Stress-strain curves of Heat H1 before (a), and after thermal aging (b), and after sodium exposure (c).

Fig. 3 shows the effect of sodium exposure where the yield stress (YS), ultimate tensile strength (UTS), and uniform elongation (UE) are plotted against exposure time. Thermal aging results were included as well for comparison. In these figures, open and solid symbols represent sodium-exposure and thermal aging results, respectively. At 550 and 600°C, thermal aging and sodium exposure decreased the YS and UTS of G91 to a similar extent, and no obvious difference can be seen between the open and close symbols. However, at 650°C, the differences between sodium-exposure and thermal aging results are pronounced. Both the YS and UTS decreased dramatically with increasing exposure time after ~1,000 h and reached a plateau at ~10,000 h after sodium exposures. The maximum reductions in the YS and UTS were >50% with sodium exposures. In contrast, thermal aging at the same temperatures only led to <15% decline in YS and UTS. Meanwhile, the UE increased after sodium exposures at 650°C, suggesting a recovery of work hardening capacity. This suggests that the specimens may have experienced decarburization in sodium at 650°C [6][7].

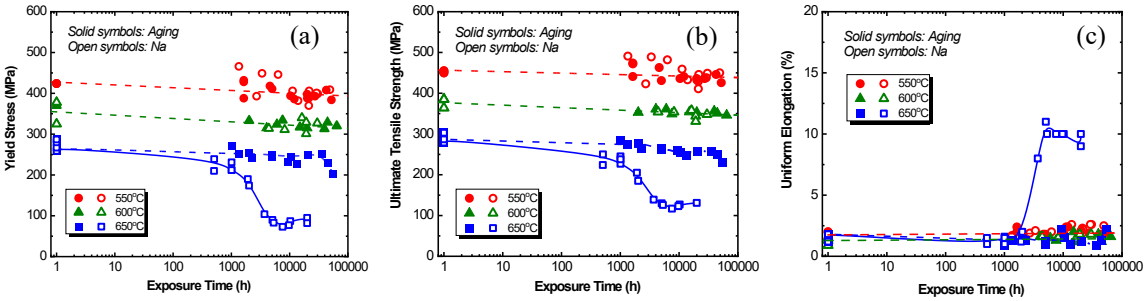

Fig. 3. Yield stress (a), ultimate tensile strength (b), and uniform elongation (c) as a function of exposure time for G91.

The change in carbon concentration in G91 resulting from sodium exposure can significantly affect its microstructural stability and mechanical properties. To understand the carburization-decarburization behavior, thermodynamic analysis was performed for the G91-sodium system. In addition to carbon concentration and temperature, three types of carbides ($M_{23}C_6$, NbC, and VC) in G91 were also taken into account in carbon activity calculation. Fig. 4 shows the calculated carbon concentration-activity relationship at three temperatures. Obviously, NbC and VC play a significant role in stabilizing carbon content in the low-carbon-activity region, essential to the decarburization resistance of G91 in sodium environment. With these results, the crossover temperature between the carburization and decarburization responses was determined and plotted in Fig. 5. While the sodium exposure at 550°C would result in carburization of G91, the exposure at 650°C would lead to decarburization in our sodium loop environment. This confirmed our mechanical results where significant differences in YS and UTS can be seen between the sodium-exposed and thermally aged samples at 650°C.

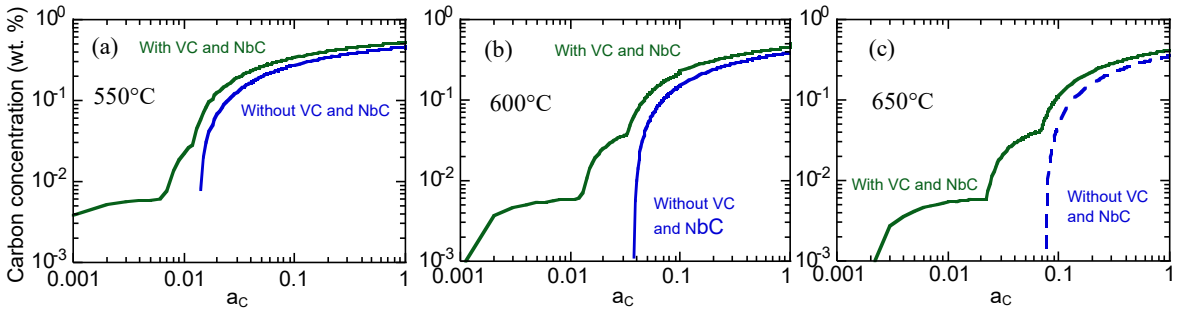

Fig. 4. Carbon concentration as a function of carbon activity in G91steel with and without VC and NbC at 550°C (a), 600°C (b), and 650°C (c)

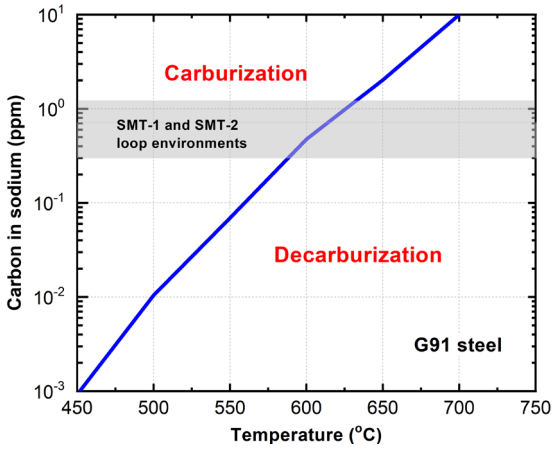

Fig. 5. Carburization-decarburization regimes of G91. The shaded area is the carbon concentration range in sodium measured in the sodium loops

CONCLUSION

Two heats of G91 steel were studied in liquid sodium at 550- 650°C to understand their corrosion behavior, microstructural evolution, and tensile properties. It was found that the YS and UTS were reduced by ~50% after sodium exposure at 650°C due to decarburization. The effect of sodium exposure at 550 and 600°C was insignificant.

To understand the carburization-decarburization behavior of G91, equilibrium carbon activity was calculated at several temperatures with three types of carbides, $M_{23}C_6$, NbC, and VC. The calculated carburization-decarburization condition implied that NbC and VC can play an important role in stabilizing the alloy's microstructure in low-carbon-activity environments, critical to the decarburization resistance of G91 in sodium environments.

REFERENCES

[1] Kazumi Aoto, Philippe Dufour, Yang Hongyi, Jean Paul Glatz, Yeong-il Kim, Yury Ashurko, Robert Hill, Nariaki Uto, "A summary of sodium-cooled fast reactor development," Progress in Nuclear Energy 77 (2014) 247-265

[2] M.C. Rowland, D. E. Plumlee, R. S. Young, "Sodium Mass Transfer: XV Behavior of Selected Steels Exposed in Flowing Sodium Test Loops," GEAP-4831, AEC-Research and Development Program, March 1965

[3] Meimei Li, Krishnamurti Natesan, and Wei-Ying, Chen, "Material Performance in Sodium," in: Konings, Rudy JM and Stoller Roger E (eds.) Comprehensive Nuclear Materials 2nd edition, vol. 4, pp. 339–356 Oxford: Elsevier (2020)

[4] R. L. Eichelberger, "The solubility of oxygen in liquid sodium: A recommended expression," AEC Research and Development Report, AI-AEC-12685, 1968.

[5] Furukawa, T., E. Yoshida, Material Performance in Sodium, in: R.J.M. Konings (Ed.) Comprehensive Nuclear Materials, Elsevier, Amsterdam, 2012, p. 327.

[6] M. Li, K. Natesan, W. Chen, Y. Momozaki, FR17: International Conference on Fast Reactors and Related Fuel Cycles: Next Generation Nuclear Systems for Sustainable Development; Yekaterinburg (Russian Federation); 26-29 Jun 2017, IAEA-CN--245-045.

[7] T. ITO, S. KATO, M. AOKI, E. YOSHIDA, T. KOBAYASHI, and Y. WADA, "Evaluation of Carburization and Decarburization Behavior of Fe-9Cr-Mo Ferritic Steels in Sodium Environments," J. Nucl. Sc. And Technol. 29 (4), 367 (1992).